Subtlety of TiO_2 phase stability: Reliability of the density functional theory predictions and persistence of the self-interaction error

Yubo Zhang, James W. Furness, Bing Xiao, and Jianwei Sun

Citation: J. Chem. Phys. **150**, 014105 (2019); doi: 10.1063/1.5055623
View online: https://doi.org/10.1063/1.5055623
View Table of Contents: http://aip.scitation.org/toc/jcp/150/1
Published by the American Institute of Physics

The Journal of Chemical Physics ARTICLE scitation.org/journal/jcp

Subtlety of TiO_2 phase stability: Reliability of the density functional theory predictions and persistence of the self-interaction error

Cite as: J. Chem. Phys. 150, 014105 (2019); doi: 10.1063/1.5055623
Submitted: 8 September 2018 • Accepted: 18 December 2018 •
Published Online: 7 January 2019

Yubo Zhang,[1] James W. Furness,[1] Bing Xiao,[2] and Jianwei Sun[1,a)]

AFFILIATIONS

[1] Department of Physics and Engineering Physics, Tulane University, New Orleans, Louisiana 70118, USA
[2] State Key Laboratory of Electric Insulation and Power Equipment, Xi'an Jiaotong University, Xi'an 710049, China

[a)] **Author to whom correspondence should be addressed:** jsun@tulane.edu

ABSTRACT

TiO_2 is an important material with broad applications that can exist in different phases with dramatically different properties. Theoretical prediction of their polymorph energetics is therefore critical for the material design and for identifying thermodynamically accessible structures. Determining TiO_2 relative phase stabilities remains challenging for first-principles methods, and density functional theory is the only approach available for studying phase stabilities at finite temperatures with acceptable computational efficiency. Here, we show that density functional theory using the recently developed efficient strongly constrained and appropriately normed (SCAN) [Sun *et al.*, Phys. Rev. Lett. **115**, 036402 (2015)] exchange-correlation functional for the first time predicts the phase stability in qualitative agreement with the experimental results at realistic conditions. Further analysis shows that the self-interaction error intrinsic in the density functional persists in the stability prediction. By correcting the self-interaction error through an empirical approach, SCAN predicts the relative stability as well as defect properties in excellent agreement with the experimental results.

INTRODUCTION

Titanium dioxide (TiO_2), a material with a wide range of applications such as dye-sensitized solar cells,[1] can exist in different phases (e.g., rutile, anatase, brookite, β-TiO_2, α-PbO_2, and baddeleyite; see Fig. S1 in supplementary material). Among them, rutile and anatase are the two phases competing to be the ground state. In the nanostructured TiO_2 employed in photovoltaics, anatase tends to be the dominant phase.[2] However, the majority of experimental studies agree that for bulk crystalline phase rutile is thermodynamically more stable than anatase.[3–5] The determination of the relative stability between anatase and rutile presents a significant challenge not only to experiments, requiring careful control of impurity concentration and synthesis conditions, but also to first-principles theoretical methods.

Within density functional theory (DFT), most exchange-correlation functionals predict the anatase phase to be more stable than rutile. The standard Perdew-Burke-Ernzerhof (PBE)[6] generalized gradient approximation (GGA) significantly over-stabilizes the anatase and brookite phases in comparison with the rutile phase.[5,7] Similar results[8] were found with the popular Heyd-Scuseria-Ernzerhof (HSE)[9,10] range-separated hybrid GGA density functional. Random phase approximation (RPA) calculations within the adiabatic-connection fluctuation-dissipation scheme[11,12] seem to have resolved the experiment-theory discrepancy, predicting rutile to be more stable than anatase by about 15 meV/formula unit. The RPA calculations were sensitive to the choice of pseudopotentials,[12] however, and were conducted non-self-consistently from the orbitals generated in DFT calculations. Furthermore, their RPA equilibrium lattice constants were determined by

calculating total RPA@X energies (X is the density functional approximation) at different unit cell volumes with the crystal structures from the corresponding DFT energy-volume calculations as structural relaxation using the RPA approach is not computationally feasible due to its prohibitive cost scaling and lack of analytic forces. Diffusion Monte Carlo (DMC) calculations,[13] a high-level yet computationally expensive electronic structure theory commonly used to benchmark DFT approximations, reverse the RPA prediction, predicting anatase as the most stable at zero temperature with degenerate rutile and brookite phases. After including zero-point energies and finite temperature contributions calculated using DFT,[13] DMC also predicts that rutile becomes more stable than anatase above 650 ± 150 K, while brookite remains the most unstable phase for all temperatures.

Here, we show that the recently developed strongly constrained and appropriately normed (SCAN) density functional[14] matches DMC predictions of the relative stability of rutile and anatase TiO_2 when zero-point vibration and finite temperature effects are considered. SCAN is computationally slightly more expensive than PBE, yet much cheaper than RPA and DMC. SCAN has been shown to be much more accurate for binary solids' relative stability than PBE.[15–17] Further analysis however shows that the self-interaction error (SIE)[18] in describing Ti-3*d* states, intrinsic to the semilocal density functionals (including PBE and SCAN), persists in the SCAN calculations. By combining a small Hubbard U[19–21] to correct the SIE, SCAN+U (*U* = 2–3 eV) predicts relative stabilities and defect properties in excellent agreement with experiments.

Figure 1 shows the transition enthalpy and transition Gibbs free energy from anatase to rutile predicted by various approaches, in comparison with the experimental results. The experimental data are rather scattered under the considered temperatures, and the latest calorimetric measurements by Smith *et al.*[5] are used as references. We first focus on the zero-temperature energetic ordering that includes the zero-point energy contribution. At T = 0 K, enthalpy [Fig. 1(a)] and Gibbs free energy [Fig. 1(b)] are equivalent. It is clear that PBE and HSE significantly over-stabilize anatase against rutile in comparison with the experiment by ~80 meV/formula unit. RPA delivers the most accurate prediction for the relative stability, likely due to its inclusion of exact exchange, that is, self-interaction free and the excellent description of van der Waals interactions. DMC largely improves over PBE and HSE although anatase is still stabilized more than rutile by about 40 meV/formula unit. Differences between the DMC data in Fig. 1 and the original DMC values in Ref. 13 are due to a further approximation made in Ref. 13 when considering the volume dependence. The SCAN value lies between those of DMC and RPA, significantly improving over that of PBE and HSE.

The finite temperature effects, which are considered by using SCAN phonon distributions (see Computational Details section and the supplementary material), are further added for the temperature-dependent transition enthalpy and transition Gibbs free energy (Fig. 1). Experimentally, the transition enthalpy stays almost constant, while the transition Gibbs free energy decreases slightly with temperature, indicating that anatase is destabilized more significantly against rutile as temperature increases. The transition enthalpy at finite temperature using the phonon density states calculated by SCAN increases with temperature, slightly off the experimental curve, while the transition Gibbs free energies from SCAN calculations decrease with temperature more strongly than the experimental data. The deviations from the experimental temperature dependence might be due to the simple harmonic approximation used for calculating phonon density states although the full study of anharmonic effects

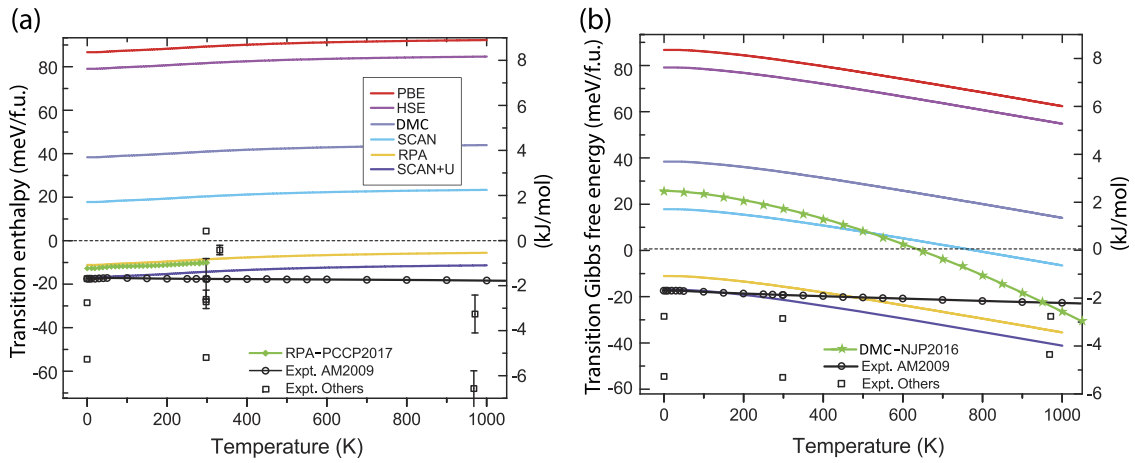

FIG. 1. (a) Transition enthalpy from the anatase phase to rutile phase $\Delta H = H^{\text{Rutile}} - H^{\text{Anatase}}$ and (b) transition Gibbs free energy from the anatase phase to rutile phase $\Delta G = G^{\text{Rutile}} - G^{\text{Anatase}}$. The green lines with solid symbols (♦ RPA-PCCP2017, ★ DMC-NJP2016) are from Refs. 12 and 13, respectively. The details of AM2009[5] and other experiments are given in Table S4 and S5. All the other solid lines are obtained by adding the zero-point and thermal effects calculated from the SCAN phonon distributions to the total internal energies from respective methods. HSE is the standard one with 25% Fock exchange.

is beyond the scope of this article. Figure 1(b) shows that SCAN matches DMC in transition Gibbs free energy,[13] predicting rutile to be more stable than anatase after about T = 750 K.

Overall, SCAN gives a reasonably good description of the relative stability and its temperature dependence, significantly improving over PBE. The PBE-GGA is constructed using only the electron density and its gradient, while SCAN belongs to the so-called meta-GGAs that add the electronic kinetic energy density as an additional ingredient. The kinetic energy density is a semilocal quantity built from the occupied orbitals immediately available in DFT calculations and thus only adds moderate extra computational cost. While different meta-GGAs have been proposed based on both non-empirical derivations[22,23] and fitting schemes,[24] SCAN is unique in that it satisfies all known 17 exact constraints applicable to a meta-GGA. By contrast, PBE only satisfies a subset of 11 exact constraints. By correctly building the kinetic energy density into a dimensionless orbital-overlap indicator, SCAN distinguishes between density regions characterizing different chemical bonds (including covalent, ionic, metallic, hydrogen, and van der Waals bonds) and treats them properly through appropriate GGA constructions, allowing SCAN to address diverse types of bonding in materials and systematically improving over PBE in general.[25]

SCAN remains a semilocal density functional, however, suffering intrinsically from the SIE as PBE does. To demonstrate SIE, Fig. 2(a) shows the energy deviation in the total energy of isolated Ti ions from the linear segments defined by the formal integer valences (i.e., +2, +3, and +4 oxidation states) with respect to fractional electron occupations.[26,27] It is seen that the most significant deviation (or error) is for the state with a 1/2 electron away from the integer valences. This is an extreme test where all semilocal density functionals must fail, and the magnitude of downward deviation demonstrates the SIE strength.[28,29] We also mention that Hartree-Fock leads to an upward deviation, and thus a hybrid functional usually reduces SIE by mixing a semilocal functional with the exact exchange. For SCAN, it also noticeably reduces SIE compared to PBE.

To resolve SIE in a true first-principles spirit, nonlocal corrections[29,30] are necessary, which are usually computationally expensive and scale poorly with system size. Note the localized orbital scaling correction developed by Yang and his collaborators represent a promising first-principles approach for correcting SIE efficiently,[31] which however is not available for solids so far. Alternatively, the empirical DFT+U[21] approach can effectively reduce SIE[32] in the underlying density functional. This method was originally developed to treat the on-site strong Coulomb repulsion between localized *d*-electrons[19–21] and has been shown to penalize the *d*-electron delocalization and effectively reduce the SIE of semilocal functionals.[32] SIE[18,26,29,33] can lead to the delocalization error,[26,27,34] which is a spurious tendency to delocalize electrons among multi-nuclei centers (e.g., Ti and O ions in TiO_2).[27] Figure 2(b) reveals that the Ti-3*d* orbitals in all the phases are fractionally occupied, with rutile and β-TiO_2 having the least and most occupations. The Hubbard correction (U = 2 eV) reduces the fractional occupancy by about 0.015 electrons for each sub-*d*-orbital of each spin and therefore effectively localizes the Ti-3*d* electrons. The corrections in energy by applying U are, for example, the weakest for rutile

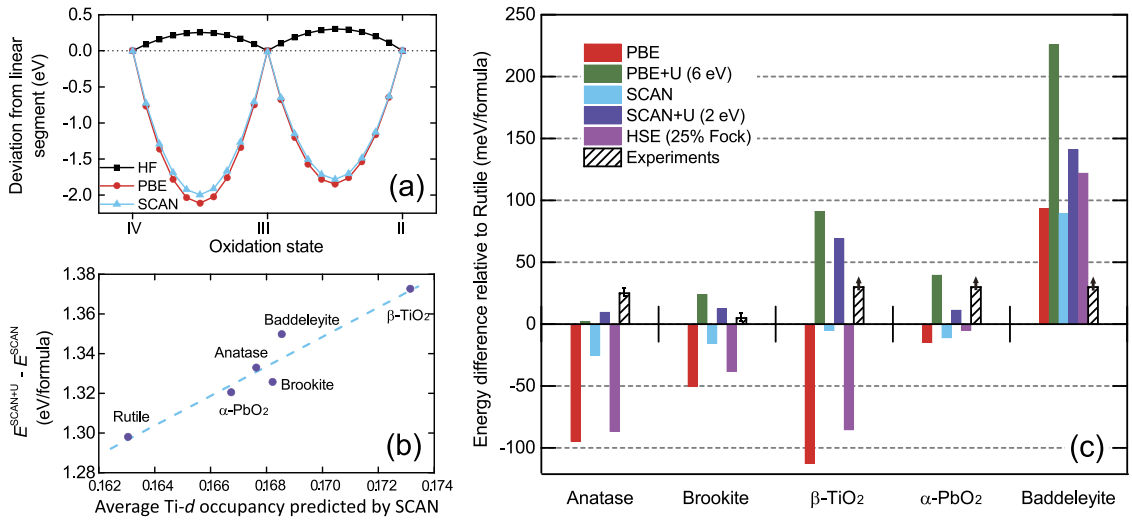

FIG. 2. (a) Deviation from the linear segment of energy as a function of occupation number of the isolated Ti ion. (b) Energetic correction by the Hubbard *U* (i.e., $E_{SCAN+U} - E_{SCAN}$, with *U* = 2 eV) with respect to the average Ti-3*d* sub-orbital occupancies (the unit is electron per sub-*d*-orbital per spin-channel), which are calculated by averaging the total 3*d* occupancy over the five Ti-*d* sub-orbitals with both spin directions. The crystal structures of the six polymorphs can be found in the supplementary material. (c) Relative stability of the six TiO_2 polymorphs from various theoretical approaches (without the zero-point energy correction), in comparison with experiments at T = 0 K.

and the strongest for β-TiO_2, forming an almost linear function in the Ti-3*d* occupations. The near-linear relation in TiO_2 solids [Fig. 2(b)] is in good accord with the deviation in Ti ions [Fig. 2(a)].

Figure 2(c) shows that the wrong energetic orderings of anatase, brookite, β-TiO_2, and α-PbO_2 with respect to rutile predicted by SCAN are reversed by the SCAN+U (U = 2 eV) approach, leading to a qualitative agreement with the experimental results. Figure 1 further shows that the transition enthalpy and Gibbs free energy from SCAN+U (U = 2 eV) match well with those experimental values for a range of temperatures. Similar results can be obtained with the PBE+U approximation though with a significantly larger U = 6 eV that can significantly degrade predictions for other properties (e.g., structural properties). The SCAN+U calculations suggest that the wrong energetic orderings from SCAN are due to the persistent delocalization error in describing the Ti-3*d* states.[35,36] In addition, the much smaller U needed by SCAN than PBE suggests that SCAN reduces SIE in comparison with PBE, consistent with the finding from the isolated Ti ion study. However, it is difficult to determine the quantitative reliability of the SCAN+*U* results since the *U* value is empirical that depends on systems and properties as further discussed below in the defect studies. Finally, we mention that the HSE06 hybrid functional with 25% Fock exact-exchange is inadequate to capture the correct energetic orderings (see the supplementary material for details).

The calculation of defect properties is another testing ground for the SCAN functional. Defects inevitably occur in a real TiO_2 sample regardless of the synthetic approach and usually play major roles for the fundamental electrical,[37,38] optical,[39] and photocatalytic[40,41] properties. Among the different types of defects, the native oxygen vacancies (V_o) can easily form during the sample preparation and, moreover, V_o vacancies near the sample surface act as active sites for the photo-induced water splitting reaction.[42] Experimentally, it is well recognized that there is an associated in-gap state 0.7–1.0 eV below the conduction band bottom of the host materials.[43–46] The conventional semilocal functionals are well-known to underestimate bandgaps [Fig. 3(a)] and thus have difficulty in localizing these defect states within the bandgap.[35] As an example, we calculate V_o (with three charge states—one neutral state V_o^0 and two charged states V_o^{1+} and V_o^{2+}) energetic levels in rutile using PBE, SCAN, SCAN+U, and HSE06 [Fig. 3(b)]. First, the energetic positions of the three V_o states are sensitively related to the local geometries of the defects, agreeing with a previous report.[47] The defect levels are dramatically changed when the geometric structures are relaxed for all considered theoretical methods. Second, the defect states cannot be localized within the bandgap predicted by PBE and SCAN after the structural relaxations. Instead, they are delocalized into the conduction bands. In contrast, the SCAN+U approach stabilizes the neutral V_o^0 state [i.e., ~0.5 eV below the conduction band minimum (CBM)] with U = 3 eV, which agrees with calculations using HSE06,[35,48] the many-body *GW* approximation,[49] and the GGA+U approach with significantly larger *U* values.[35,46,50,51]

Consistent with the stability calculations, the Hubbard U in the DFT+U approach is used here to reduce SIE. Unfortunately, the energetic positions of the three V_o states from the DFT+U approach remain ambiguous due to the empiricism in U. The SCAN+U approach with U = 2 eV, which yields the best agreement with the experimental transition Gibbs free energy [Fig. 1(b)], cannot stabilize the V_o^0 gap states after the structural relaxation: U = 2 eV yields a bandgap not large enough such that the V_o^0 gap state merges with the conduction bands

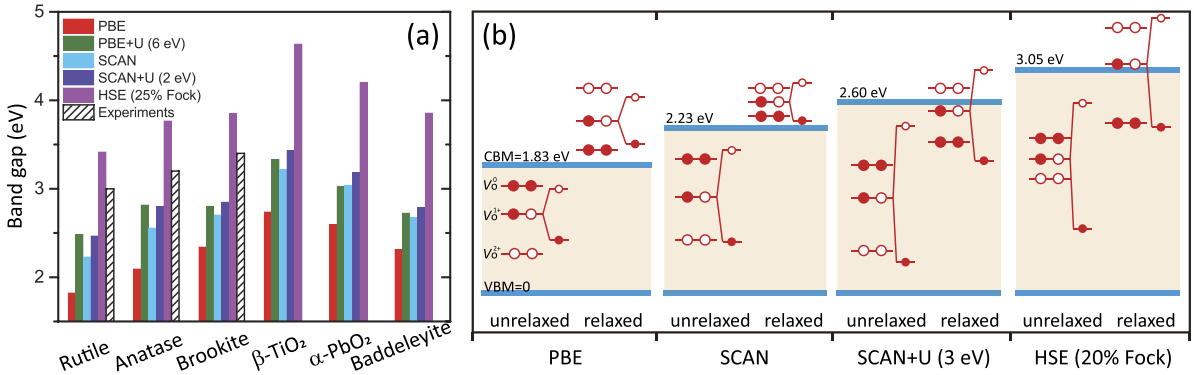

FIG. 3. (a) Bandgaps of the six TiO_2 polymorphs predicted by various theoretical approaches, in comparison with available experimental optical measurements (rutile ~3.0 eV,[52,53] anatase ~3.2 eV,[53] and brookite ~3.27 eV[54]). (b) Theoretically predicted energetic levels of the oxygen vacancy (V_o) in the rutile TiO_2. The results are compared for both relaxed and unrelaxed structures when one oxygen atom is removed from a 72-atom supercell. V_o^0 (identified as two dots) is the neutral state, and V_o^{1+} (identified as one dot and one open circle) and V_o^{2+} (identified as two open circles) are charged states simulated by taking one and two electrons away from the supercell, respectively. For the V_o^{1+} state, the energetic positions are given for both up and down spin channels. For the states merged with the conduction bands, their energetic positions are estimated according to the projected density of states of the three nearest-neighbor Ti ions.[47] Note that *U* = 2 eV in the SCAN+*U* and 25% Fock exact-exchange in HSE06 are used for the bandgap calculations, but their values are 3 eV and 20%[47] for the defect level calculations, respectively. VBM is the valence band maximum, and CBM is the conduction band minimum.

(not shown here) although the qualitative agreement is found for the V_O^{1+} and V_O^{2+} defect states. Instead, U = 3 eV is used to reproduce all three defect states in Fig. 3(b). However, SCAN+U (U = 3 eV) overcorrects the transition enthalpy from the anatase phase to the rutile phase by about 18 meV/formula too negative in comparison with the experimental data, while SCAN has an error of about 40 meV/formula too positive, as shown in Fig. 1(a). It is worth noting that the global hybrid HSE06 has a similar empiricism for the mixing fraction of the Fock exact-exchange (see the supplementary material for details).

In summary, after considering the zero-point and finite temperature effects through phonon calculations, SCAN predicts the TiO_2 rutile phase is more stable than the anatase phase around T = 750 K, consistent with the condition for experimentally synthesizing rutile from anatase. By correcting the intrinsic SIE through the empirical Hubbard U, SCAN predicts transition Gibbs free energies that match well with experimental values for a range of temperatures. However, the empiricism in the SCAN+U approach means the TiO_2 phase stability and related problems remain a puzzle to theoretical methods and demands developments in non-empirical corrections for treating SIE.

COMPUTATIONAL DETAILS

The electronic structures are calculated using the Vienna *Ab initio* Simulation Package (VASP).[55,56] We use the projector augmented-wave (PAW) potentials for TiO_2 and Ti-3*s*/3*p* semicore electrons are taken as valence states. For comparison, we consider three exchange-correlation functionals: the standard PBE-GGA,[6] the hybrid functional HSE06,[10] and the recently developed SCAN *meta*-GGA.[14] The plane-wave energy cutoff is 600 eV for both the semilocal functionals PBE and SCAN, but a smaller value of 500 eV is used for HSE06 to reduce the computational scale. The DFT+U with an empirical Hubbard U is combined with the semilocal functionals to reduce SIE. Whereas HSE06 includes 25% Fock exact-exchange by default, the mixing fraction can also be changed in, for example, calculating defect properties.[47] The positively charged defect states are simulated by extracting background electrons from the systems. Crystal structures are fully relaxed unless specified.

For the transition enthalpy (ΔH) and transition Gibbs free energy (ΔG), the contributions of zero-point energy and finite temperature effects are estimated through calculating the vibrational properties. The supercell approach (also called frozen-phonon approach) is used to simulate the phonon properties. We use the Phonopy code[57] to generate the finite atomic displacements, calculate the harmonic force constants, and finally produce the key information of phonon frequency ω_q (q is the wave vector). VASP is used as the external force calculator. Thermal properties of Helmholtz free energy (A) and entropy (S) are then easily obtained,

$$A = \frac{1}{2}\sum_{q,s}\hbar\omega(q,s) + k_B T\sum_{q,s}\ln[1-\exp(-\frac{\hbar\omega(q,s)}{k_B T})],$$

$$S = -k_B T\sum_{q,s}\ln\left[1-\exp\left(-\frac{\hbar\omega(q,s)}{k_B T}\right)\right] - \frac{1}{T}\sum_{q,s}\frac{\hbar\omega(q,s)}{\exp(\hbar\omega(q,s)/k_B T)-1},$$

where s is the band index and k_B is the Boltzmann constant. The zero-point energy is included within the Helmholtz free energy A. After doing further data processing, we get the enthalpy (defined as $H = A + TS$) and Gibbs free energy (defined as $G = H - TS + PV$, with the PV term being safely ignored). Note that the DFT energies (i.e., the internal energy U) should be included in deriving the enthalpy H.

The harmonic approximation is assumed in the above thermal property calculations and, in principle, the finite temperature effect should be better estimated at the quasi-harmonic level to also consider the thermal expansion effect. But, the latter approach is more computationally expensive. Another technical difficulty is that the deformed crystal structures due to thermal effects can have (false) imaginary frequencies [see Fig. S2], an intrinsic problem for the quasi-harmonic approximation.[58]

SUPPLEMENTARY MATERIAL

See supplementary material for crystal structures (CIF); calculated lattice constants in comparison with experiments, bandgap, collection of experimental transition enthalpy and transition Gibbs free energy, calculated formation enthalpy, phonon dispersion relation, and evaluation of the Fock exact-exchange in HSE06 (PDF).

ACKNOWLEDGMENTS

This work was supported by the start-up funding from Tulane University, by the U.S. DOE, Office of Science, Basic Energy Sciences Grant No. DE-SC0235021(core research), and by the National Energy Research Scientific Computing Center supercomputing center. Calculations were partially performed using the Cypress cluster at Tulane University, and we thank Hoang Tran, Carl Baribault, and Hideki Fujioka for their computational support.

REFERENCES

[1] J. Nowotny, *Oxide Semiconductors for Solar Energy Conversion: Titanium Dioxide* (CRC Press, Boca Raton, 2011).
[2] V. Shklover, M.-K. Nazeeruddin, S. Zakeeruddin, C. Barbe, A. Kay, T. Haibach, W. Steurer, R. Hermann, H.-U. Nissen, and M. Grätzel, Chem. Mater. **9**, 430 (1997).
[3] M. Ranade, A. Navrotsky, H. Zhang, J. Banfield, S. Elder, A. Zaban, P. Borse, S. Kulkarni, G. Doran, and H. Whitfield, Proc. Natl. Acad. Sci. U. S. A. **99**, 6476 (2002).
[4] A. A. Levchenko, G. Li, J. Boerio-Goates, B. F. Woodfield, and A. Navrotsky, Chem. Mater. **18**, 6324 (2006).
[5] S. J. Smith, R. Stevens, S. Liu, G. Li, A. Navrotsky, J. Boerio-Goates, and B. F. Woodfield, Am. Mineral. **94**, 236 (2009).
[6] J. P. Perdew, K. Burke, and M. Ernzerhof, Phys. Rev. Lett. **77**, 3865 (1996).

[7]F. Labat, P. Baranek, C. Domain, C. Minot, and C. Adamo, J. Chem. Phys. **126**, 154703 (2007).
[8]M. T. Curnan and J. R. Kitchin, J. Phys. Chem. C **119**, 21060 (2015).
[9]J. Heyd, G. E. Scuseria, and M. Ernzerhof, J. Chem. Phys. **118**, 8207 (2003).
[10]A. V. Krukau, O. A. Vydrov, A. F. Izmaylov, and G. E. Scuseria, J. Chem. Phys. **125**, 224106 (2006).
[11]C. E. Patrick and K. S. Thygesen, Phys. Rev. B **93**, 035133 (2016).
[12]Z.-H. Cui, F. Wu, and H. Jiang, Phys. Chem. Chem. Phys. **18**, 29914 (2016).
[13]Y. Luo, A. Benali, L. Shulenburger, J. T. Krogel, O. Heinonen, and P. R. Kent, New J. Phys. **18**, 113049 (2016).
[14]J. Sun, A. Ruzsinszky, and J. P. Perdew, Phys. Rev. Lett. **115**, 036402 (2015).
[15]Y. Hinuma, H. Hayashi, Y. Kumagai, I. Tanaka, and F. Oba, Phys. Rev. B **96**, 094102 (2017).
[16]Y. Zhang, D. A. Kitchaev, J. Yang, T. Chen, S. T. Dacek, R. A. Sarmiento-Pérez, M. A. Marques, H. Peng, G. Ceder, and J. P. Perdew, npj Comput. Mater. **4**, 9 (2018).
[17]C. Shahi, J. Sun, and J. P. Perdew, Phys. Rev. B **97**, 094111 (2018).
[18]J. P. Perdew and A. Zunger, Phys. Rev. B **23**, 5048 (1981).
[19]A. Liechtenstein, V. Anisimov, and J. Zaanen, Phys. Rev. B **52**, R5467 (1995).
[20]S. L. Dudarev, G. A. Botton, S. Y. Savrasov, C. J. Humphreys, and A. P. Sutton, Phys. Rev. B **57**, 1505 (1998).
[21]I. A. Vladimir, F. Aryasetiawan, and A. I. Lichtenstein, J. Phys.: Condens. Matter **9**, 767 (1997).
[22]J. Tao, J. P. Perdew, V. N. Staroverov, and G. E. Scuseria, Phys. Rev. Lett. **91**, 146401 (2003).
[23]J. Sun, B. Xiao, and A. Ruzsinszky, J. Chem. Phys. **137**, 051101 (2012).
[24]Y. Zhao and D. G. Truhlar, J. Chem. Phys. **125**, 194101 (2006).
[25]J. Sun, R. C. Remsing, Y. Zhang, Z. Sun, A. Ruzsinszky, H. Peng, Z. Yang, A. Paul, U. Waghmare, X. Wu, M. L. Klein, and J. P. Perdew, Nat. Chem. **8**, 831 (2016).
[26]J. P. Perdew, A. Ruzsinszky, G. I. Csonka, O. A. Vydrov, G. E. Scuseria, V. N. Staroverov, and J. Tao, Phys. Rev. A **76**, 040501 (2007).
[27]A. Ruzsinszky, J. P. Perdew, G. I. Csonka, O. A. Vydrov, and G. E. Scuseria, J. Chem. Phys. **125**, 194112 (2006).
[28]P. Mori-Sánchez, A. J. Cohen, and W. Yang, J. Chem. Phys. **125**, 201102 (2006).
[29]A. J. Cohen, P. Mori-Sánchez, and W. Yang, Science **321**, 792 (2008).
[30]M. R. Pederson, A. Ruzsinszky, and J. P. Perdew, J. Chem. Phys. **140**, 121103 (2014).
[31]C. Li, X. Zheng, N. Q. Su, and W. Yang, Natl. Sci. Rev. **5**, 203 (2017).
[32]M. Cococcioni and S. de Gironcoli, Phys. Rev. B **71**, 035105 (2005).
[33]J. P. Perdew, R. G. Parr, M. Levy, and J. L. Balduz, Phys. Rev. Lett. **49**, 1691 (1982).
[34]P. Mori-Sánchez, A. J. Cohen, and W. Yang, Phys. Rev. Lett. **100**, 146401 (2008).
[35]E. Finazzi, C. Di Valentin, G. Pacchioni, and A. Selloni, J. Chem. Phys. **129**, 154113 (2008).
[36]B. J. Morgan and G. W. Watson, J. Phys. Chem. C **114**, 2321 (2010).
[37]L. Forro, O. Chauvet, D. Emin, L. Zuppiroli, H. Berger, and F. Lévy, J. Appl. Phys. **75**, 633 (1994).
[38]M. K. Nowotny, T. Bak, and J. Nowotny, J. Phys. Chem. B **110**, 16270 (2006).
[39]V. M. Khomenko, K. Langer, H. Rager, and A. Fett, Phys. Chem. Miner. **25**, 338 (1998).
[40]J. Nowotny, T. Bak, M. K. Nowotny, and L. R. Sheppard, Int. J. Hydrogen Energy **32**, 2609 (2007).
[41]J. Nowotny, T. Bak, M. K. Nowotny, and L. R. Sheppard, Int. J. Hydrogen Energy **32**, 2630 (2007).
[42]R. Schaub, P. Thostrup, N. Lopez, E. Lægsgaard, I. Stensgaard, J. K. Nørskov, and F. Besenbacher, Phys. Rev. Lett. **87**, 266104 (2001).
[43]R. L. Kurtz, R. Stock-Bauer, T. E. Msdey, E. Román, and J. De Segovia, Surf. Sci. **218**, 178 (1989).
[44]M. A. Henderson, W. S. Epling, C. H. Peden, and C. L. Perkins, J. Phys. Chem. B **107**, 534 (2003).
[45]V. E. Henrich, G. Dresselhaus, and H. Zeiger, Phys. Rev. Lett. **36**, 1335 (1976).
[46]M. Nolan, S. D. Elliott, J. S. Mulley, R. A. Bennett, M. Basham, and P. Mulheran, Phys. Rev. B **77**, 235424 (2008).
[47]A. Janotti, J. B. Varley, P. Rinke, N. Umezawa, G. Kresse, and C. G. Van de Walle, Phys. Rev. B **81**, 085212 (2010).
[48]A. Janotti and C. G. Van de Walle, Phys. Status Solidi (b) **248**, 799 (2011).
[49]A. Malashevich, M. Jain, and S. G. Louie, Phys. Rev. B **89**, 075205 (2014).
[50]C. J. Calzado, N. C. Hernández, and J. F. Sanz, Phys. Rev. B **77**, 045118 (2008).
[51]J. Stausholm-Møller, H. H. Kristoffersen, B. Hinnemann, G. K. H. Madsen, and B. Hammer, J. Chem. Phys. **133**, 144708 (2010).
[52]A. Amtout and R. Leonelli, Phys. Rev. B **51**, 6842 (1995).
[53]L. Kavan, M. Grätzel, S. Gilbert, C. Klemenz, and H. Scheel, J. Am. Chem. Soc. **118**, 6716 (1996).
[54]A. Mattsson and L. Osterlund, J. Phys. Chem. C **114**, 14121 (2010).
[55]G. Kresse and J. Furthmüller, Phys. Rev. B **54**, 11169 (1996).
[56]G. Kresse and J. Furthmüller, Comput. Mater. Sci. **6**, 15 (1996).
[57]A. Togo and I. Tanaka, Scr. Mater. **108**, 1 (2015).
[58]O. Hellman, I. Abrikosov, and S. Simak, Phys. Rev. B **84**, 180301 (2011).